Prolonged flooding followed by drying increase greenhouse gas emissions differently from soils under grassland and arable land uses

Guo, Yafei; Saiz, Ernesto; Radu, Aleksandar; Sonkusale, Sameer; Ullah, Sami

DOI:
10.1016/j.geodrs.2023.e00697

Document Version
Publisher's PDF, also known as Version of record

Citation for published version (Harvard):
Guo, Y, Saiz, E, Radu, A, Sonkusale, S & Ullah, S 2023, 'Prolonged flooding followed by drying increase greenhouse gas emissions differently from soils under grassland and arable land uses', *Geoderma Regional*, vol. 34, e00697. https://doi.org/10.1016/j.geodrs.2023.e00697

Geoderma Regional 34 (2023) e00697

Contents lists available at ScienceDirect

Geoderma Regional

journal homepage: www.elsevier.com/locate/geodrs

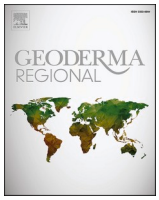

Prolonged flooding followed by drying increase greenhouse gas emissions differently from soils under grassland and arable land uses

Yafei Guo [a,1,*], Ernesto Saiz [b,1], Aleksandar Radu [c], Sameer Sonkusale [d], Sami Ullah [a,*]

[a] School of Geography, Earth and Environmental Sciences, University of Birmingham, Birmingham B15 2TT, UK
[b] School of Health and Life Sciences, Teesside University, Middlesbrough TS1 3BX, UK
[c] School of Chemistry, University of Lincoln, Lincoln LN6 7TS, UK
[d] School of Engineering, Tufts University, Medford, MA 02155, USA

ARTICLE INFO

Keywords:
Prolonged flooding
Flooding-drying
Arable soil
Grassland soil
Greenhouse gas
Net zero greenhouse gas emissions

ABSTRACT

Several climate change scenarios have predicted that heavy precipitation could result in prolonged flooding (PF) and flooding–drying (FD) of soils under agriculture. The influence of PF and FD on soil greenhouse gas (GHG) fluxes and ammonium-nitrogen (NH_4^+-N) and nitrate-nitrogen (NO_3^--N) dynamics of arable and grassland soils, the dominant land-use types in the UK, remain unclear. A two-month soil incubation experiment was conducted to determine the impact of PF and FD on soil N dynamics and GHG fluxes from arable and grassland soils. Arable soil emitted more N_2O-N when soil moisture exceeded 100% water-holding capacity (WHC) compared to grassland soil under PF. Grassland soils exhibited increased N_2O-N emissions than arable soils when soil moisture was lower than 100% WHC under FD. When soil moisture exceeded 100% WHC, the available NO_3^--N in the soil contributed 58% of N_2O-N emissions potentially by denitrification from grassland. When soil moisture was lower than 100% WHC, soil NH_4^+-N and NO_3^--N contributed 71% of N_2O-N emissions, which suggests coupling of nitrification-denitrification processes in driving high emissions from grassland soils. The N_2O-N and CO_2-C emissions increased with the incubation time under FD. Moreover, FD significantly increased N_2O-N, CO_2-C, and CH_4-C emissions in grassland soil by 0.93, 2.15, and 37.29 times more than arable soil, respectively. These findings points to important tipping points in the source strengths of GHG fluxes from the two land use types differently. Future land use changes should consider the contribution of the changing dynamics of GHG fluxes in light of climate extremes and its implications for net zero greenhouse gas emission ambitions.

1. Introduction

Carbon dioxide (CO_2), methane (CH_4), and nitrous oxide (N_2O) are the primary greenhouse gases (GHGs) present in the Earth's atmosphere (IPCC, 2022). The atmospheric CO_2 concentration has increased to approximately 420 ppm and future rapid increase is expected to reach 550 ppm by mid-century and 1000 ppm by the end of this century (IPCC, 2022). The N_2O is a long-lived GHG with a long-term global warming potential 300 times greater than CO_2 (Carneiro et al., 2010) and is a strong stratospheric ozone-depleting substance (Thompson et al., 2019). The N_2O concentration in the atmosphere has also risen steadily since the mid-twentieth century (IPCC, 2022), from approximately 290 ppb in 1940 to 330 ppb in 2017 (Park et al., 2012). The atmospheric CH_4 continues to rise at a rate of approximately 22 Tg every year, as global sources are larger than sinks (IPCC, 2001). Agricultural soils are important source of GHGs (Liu et al., 2019). They are considered the main source of non-CO_2 anthropogenic GHG and are responsible for 78.6% of N_2O and 39.1% of CH_4 emissions worldwide (IPCC, 2022). The increasing atmospheric GHG concentrations are inducing changes in climate including shifts in the intensity and duration of precipitation that are very likely to feedback into the production and emission of GHG (IPCC, 2022).

Nitrogen (N) is a necessary nutrient in agricultural ecosystems (Fixon and West, 2002) as it is critical for plant growth (Gilsanz et al., 2016); however, the nitrogen use efficiency of applied fertilizer N by plants is <40% (Chen et al., 2008). In agricultural soils, the applied fertilizer N

* Corresponding authors.
E-mail addresses: y.guo.8@bham.ac.uk (Y. Guo), E.SaizVal@tees.ac.uk (E. Saiz), ARadu@lincoln.ac.uk (A. Radu), sameer@ece.tufts.edu (S. Sonkusale), s.ullah@bham.ac.uk (S. Ullah).
[1] These authors contributed equally: Yafei Guo and Ernesto Saiz.

https://doi.org/10.1016/j.geodrs.2023.e00697
Received 27 February 2023; Received in revised form 20 June 2023; Accepted 22 August 2023
Available online 23 August 2023

contributes to N_2O emissions. The N_2O can be produced from several biological processes, including nitrification, denitrification, codenitrification, dissimilatory nitrate reduction to ammonia, and chemo denitrification, which involve different microbial groups in soil (Harter et al., 2014). The two main microbial processes that produce N_2O are nitrification and denitrification (Hu et al., 2015; Sgouridis and Ullah, 2017). Nitrifying microbes undertake biological oxidation of ammonium (NH_4^+) to nitrite (NO_2^-) and further to nitrate (NO_3^-) and can produce N_2O by nitrification under aerobic soil conditions (Wrage et al., 2001). Denitrifying microbes reduce NO_3^- to NO_2^-, nitric oxide (NO^-), N_2O, and molecular nitrogen (N_2) by denitrification under anaerobic conditions (Köster et al., 2013). The majority of naturally occurring emissions of CH_4 can be attributed to the biogenic processes of methanogens (methane-emitting microorganisms), as a final step in the anaerobic decomposition of organic matter (Gütlein et al., 2018). These microorganisms are predominant in anaerobic areas rich in organic carbon (Conrad, 2009). Carbon dioxide emissions come from the soil mineralization of soil organic carbon (SOC) (Guo et al., 2019). In intact soil systems where plants are present, CO_2 emissions originate from both microbial and plant respiration.

Soil CO_2, N_2O, and CH_4 exchanges are driven by aerobic (when soil moisture (SM) was lower) and anaerobic (when SM was higher) microbial processes (Gütlein et al., 2018), which are in turn influenced by soil properties and environmental factors (temperature, precipitation), soil physical (texture and oxygen concentration) and chemical properties (pH and nutrient availability) (Miller et al., 2020). Soil pH manipulates the microbial community structure, and therefore, the decomposition or accumulation of SOC (Malik et al., 2018) to influence the GHG emissions.

Land-use change affects soil GHG emissions due to changes in vegetation, soil hydrology, and nutrient management (Gütlein et al., 2018). Grassland dominates the landscape in the United Kingdom (40%) (Caroline et al., 2017). A total of 56,506 km^2 of land is classed as arable and 96,949 km^2 is classed as grasslands (improved, neutral, calcareous, and acid) in the UK (Rowland et al., 2017). Moreover, GHG emissions from soils are also linked to the hydrological conditions, with deep water tables favouring CO_2 emissions, shallow water tables (less than ~20 cm) favouring CH_4 emissions, and fluctuating water tables potentially being conducive to N_2O emissions (Petersen et al., 2012; Poyda et al., 2016; Wilson et al., 2016).

Climate change is predicted to cause major changes in precipitation patterns with increased frequency and intensity of large rainfall events (IPCC, 2007). Flooding–drying (FD) cycles of soil may expose unavailable (physically protected) soil organic matter to microbes through breakdown of soil aggregates (Zhang et al., 2020) as well as changing the redox conditions in soils with implications for shifts in net N_2O, CH_4, and CO_2 emissions into the atmosphere. Changes in flooding frequency of soils following future climate change will likely affect the timing and magnitude of N_2O emissions from the soil to the atmosphere (Jørgensen and Elberling, 2012). Production and emission of GHGs may vary depending on soil physical properties, SM status as influenced by precipitation under climate change extremes (Fay et al., 2010), and fertilization (Mazza et al., 2018). Therefore, changes in soil saturation following extreme precipitation events in the future are likely to change the timing and extent of GHG emissions from soils. In fact, soil saturation is more likely to be severe in agricultural soils, where precipitation interception is low compared with forest soils.

In this study, we conducted an incubation experiment to identify the effect of prolonged flooding (PF) and FD (extreme SM condition) of soils on soil N_2O-N, CO_2-C and CH_4-C emissions and NH_4^+-N and NO_3^--N dynamics under grassland and arable land uses. We hypothesized that: (1) arable soil will result in high N_2O-N, CO_2-C and CH_4-C emissions and GWP under PF and FD due to high N fertilizer addition; and (2) FD will lead to high N_2O-N, CO_2-C and CH_4-C emissions and GWP in grassland and arable soil due to faster mineralization of soil organic matter. The objectives of this study were to determine soil N_2O-N, CO_2-C, and CH_4-C emissions as influenced by environmental (flooding and draining) and edaphic factors (NH_4^+, NO_3^-, and total dissolved nitrogen contents) in fertilized grassland and arable soil in the UK. The result could help us to understand the GHG emissions after conversion of arable land use to grasslands (in order to improve soil health and sequester carbon) under climate change scenarios (heavy rain).

2. Materials and methods

2.1. Study site description and soil collection

Soil samples were taken by a soil auger (core sampler) (up to10 cm) from an experimental demonstration mixed land use farm at Honeydale Farm (51°51′N, 1°35′W), located in the Evenlode Valley in the heart of the Cotswolds, UK. Honeydale Farm is a 107-acre (43 ha) farm. The nearest climate station is Little Rissington (51°51′N, 1°41′W) which is 8 miles away. The annual monthly maximum temperature is 13.41 °C and monthly minimum temperature is 5.89 °C. Air frost occurs 46.14 days of the year. The cumulative number of sunshine hours is 1631.53 and the average rainfall is 809.63 mm per year. Monthly mean wind speed at 10 m is 10.30 knots. General cropping is over chalk; spring and autumn cereals can be grown. The poor SM is likely to be the main limiting factor on crop yield (Cranfield soil and agrifood institute, 2023).

Grassland soil was restored for 4 years with 'HERBAL' (Cotswold Grass Seeds, Cotswold Business Village, Moreton-in-Marsh, UK) grazing ley and used for grazing. Previously, the land was used for arable cultivation (wheat and oats) over years for decades before changing to grass. HERBAL all-round mixture (20 species) provides wholesome and substantial forage for grazing and occasional cutting. It can also provide grazing for early turnout and continues to produce forage right through the summer and autumn. Containing deep-rooting ingredients, this ley not only improves soil structure but also draws up essential vitamins and minerals for the ruminant animal (https://www.cotswoldseeds.com/products/542/herbal-grazing-ley-four-year-drought-resistant-ley). The arable soil was a control plot with winter wheat planted in October. The soil N fertilization rate in the Honeydale farm ranges between 120 and 150 kg N per ha depending on the year of production in light of N fertilization rates recommended by DEFRA. This soil has been under wheat or barley cultivation for 30 years. The parent material of both the grassland and arable soil is Oolitic limestone. Arable soil and grassland soil are inceptisols (Soil Taxonomy-USDA).

Soil samples were carefully collected from 0 to 20 cm soil depth from the grassland and arable plots on May 18, 2022 (around 20 soil samples were taken in both grassland and arable plots and then mixed to give one grassland and one arable soil sample). Fresh soil samples were stored in a refrigerator at 4 °C after the removal of plant residues and stones and passing through a 2-mm sieve for homogenization. The main soil

Table 1
Selected soil physical and chemical properties before the experiment. TOC is total dissolved organic carbon, TDN is total dissolved nitrogen, TC is total carbon, TN is total nitrogen, and WHC is water-holding capacity. Means of the same index and indicated by the same lower-case letter are not significantly different at $P < 0.05$ on the basis of Tukey's HSD test.

Soil type	NH_4^+-N mg kg^{-1}	NO_3^--N mg kg^{-1}	TOC-C mg kg^{-1}	TDN-N mg kg^{-1}	TC g kg^{-1}	TN g kg^{-1}
Grassland	0.63a (±0.07)	10.03a (±0.76)	88.67b (±1.10)	22.82a (±0.26)	69.81b (±0.95)	4.22b (±0.13)
Arable	0.34a (±0.06)	277.28b (±4.65)	61.49a (±1.76)	254.19b (±4.24)	53.88a (±0.58)	3.71a (±0.21)
Soil type	Clay (%)	Silt (%)	Sand (%)	pH	WHC (%)	C/N
Grassland	46.54a (±0.47)	33.23a (±0.70)	20.23b (±1.01)	7.36b (±0.04)	72.42a (±0.44)	16.66a (±0.39)
Arable	46.12a (±0.74)	39.45b (±0.86)	14.43a (±0.80)	6.90a (±0.01)	70.52a (±0.21)	14.95a (±0.98)

Note: Average value (± relative standard deviation), $n = 4$.

properties are given in Table 1.

2.2. Incubation experiment

Grassland and arable soils were each packed into a 1 L Mason Jar pot to achieve a bulk density of 0.9 g cm^{-3} (field bulk density) with a 10 cm height. Three replications were set for each land use type.

All pots were fertilized with 100 mg NH_4^+-N kg^{-1} soil (180 kg NH_4^+-N ha^{-1}) using ammonium sulphate salt ($(NH_4)_2SO_4$) in order to determine the response of fertilized soils to saturation. Deionized water was added to keep SM at 110% water-holding capacity (WHC) and the pots were incubated for 4 weeks. Soil moisture was kept constant by weighing the pot each day to simulate PF (Fig. 1).

All pots were fertilized with 100 mg NH_4^+-N kg^{-1} soil again using $(NH_4)_2SO_4$ after 4 weeks of incubation under PF. This was followed by adjustment of moisture to 130% WHC for 4 weeks to mimic another intense precipitation event. Water loss (e.g., evaporation) was not replaced over time to simulate drying following flooding (FD) (Fig. 1).

2.3. Collection and measurement of GHGs

The CO_2-C, N_2O-N, and CH_4-C emission rates were calculated by measuring the concentration of these gases in the headspace of closed pots at different times. The CO_2-C, N_2O-N, and CH_4-C samples were collected once a day during the first week, once per two days during the second week, and once per three days during the last two weeks (Guo et al., 2021a). The pots were first closed by adding lids, gases were mixed by collecting and injecting the gas in and out of the pots a few times with a syringe, and then samples were collected from the headspace at 0, 30, and 60 min after lid closure (Guo et al., 2021b). A 20-ml syringe and hypodermic needle was used to collect the gas samples and inject them into pre-evacuated 12-ml glass headspace exetainer vials fitted with a chloro-butyl rubber septum (Guo et al., 2022a). Gas sampling was carried out between 09:00 and 10:00 a.m. The pots were left open outside of the sampling periods.

The concentrations of CO_2-C, N_2O-N, and CH_4-C in the 12-ml glass exetainer vials were measured by gas chromatography (Agilent 7890A GC, Agilent, CA, USA). An electron capture detector (ECD) was used to detect the N_2O, with a temperature of 350 °C and an N_2 as carrier gas. A flame ionization detector (FID) was used to detect the CH_4 and CO_2 concentrations, with a temperature of 250 °C and N_2 as the carrier gas. The CH_4 was eluted and analysed first. Secondly, CH_4 (equal to CO_2) was analysed after the sample was passed through a methanizer to convert the CO_2 to CH_4 for detection.

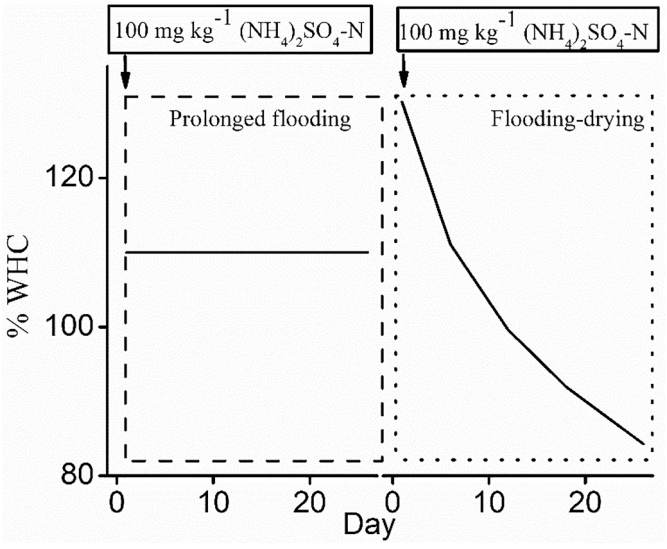

Fig. 1. Soil water content as percentage water-holding capacity (WHC) during the prolonged flooding and flooding–drying incubation.

Total CO_2-C, N_2O-N, and CH_4-C emissions during the experimental period were calculated from the daily emissions of the gases (Guo et al., 2022b). We used the fluxes of CO_2-C, N_2O-N, and CH_4-C multiplied by the number of hours during sampling (24 h in the first week, 48 h in the second week, and 72 h in the last six weeks) then added them together to obtain the total emissions (mg kg^{-1} or μg kg^{-1}). The global warming potential (GWP) was used to quantitatively assess the relative impacts of N_2O, CH_4, and CO_2 on climate change by summing the 100-year radiative forcing associated with each of the three measured GHGs (Hawthorne et al., 2017). The conversion factors for the assessment of GWP for soil N_2O, CH_4, and CO_2 are 298, 25, and 1 respectively (IPCC, 2021). The GWP was calculated as follows:

$$GWP = Total_{CO_2} \times 1 + Total_{CH_4} \times 25 + Total_{N_2O} \times 298 \quad (1)$$

where $Total_{CO_2}$ is the total emissions of CO_2, $Total_{CH_4}$ is the total emissions of CH_4, and $Total_{N_2O}$ is the total emissions of N_2O.

2.4. NH_4^+-N and NO_3^--N measurement

Three types (available, labile and stable) of NH_4^+-N and NO_3^--N in soil were selected to determine their influence on GHG emissions. The NH_4^+-N and NO_3^--N in pore water (WNH_4 and WNO_3) are available for soil microbes to use since they are present in the pore water. The NH_4^+-N and NO_3^--N in 0.5 M HCl from ion-exchange resin membranes (IERM) (INH_4 and INO_3) are labile for soil microbes to use. The NH_4^+-N and NO_3^--N in 2 M KCl from soil extraction (SNH_4 and SNO_3) are stable for soil microbes to use.

2.4.1. Soil pore water collection

Ten millilitres of soil pore water were collected once a day during the first week, once per two days during the second week, and once per three days during the last two weeks under PF. The samples were collected once a day during the first week, and once per two days during the first two weeks under FD (the pore water was collected in the FD treatment when the SM was higher than 100% WHC, SM >100%WHC). The pore water was collected via a fibre microfluidic thread.

2.4.2. Ion-exchange resin membranes

The IERMs included anion-exchange membranes (AEMs) that sorb NO_3^--N and cation-exchange membranes (CEMs) that sorb NH_4^+-N from soil pore water through diffusion. These membranes were inserted into a 7.5 cm depth of soil for passive sensing of the mineral N during the course of the incubation. The CEM and AEM (SNOWPURE, San Clemente, CA, USA) were put in the deionized water for 48 h at 90 °C, followed by drying the membrane. The CEM was saturated with H^+ by leaving CEM strips overnight in 2 M HCl. The AEM was saturated with HCO_3^- by leaving the AEM strips overnight in 1 M $NaHCO_3$. IERMs were rinsed free of excess HCl and $NaHCO_3$ with deionized water. A further 24-h equilibration and removal of the chemicals with deionized water was required for the CEM and AEM. Prepared strips were kept moisturized in sealed plastic bags prior to installation. The CEM and AEM were inserted into the soil and replaced each week. The IERMs were carefully rinsed with deionized water until all traces of soil were removed. Desorption of ions was achieved by shaking each strip (cations and anions separated) for 2 h in 17.5 ml of 0.5 M HCl at 200 rpm.

2.4.3. Soil extraction

Subsoil samples were collected to a depth of 10 cm on Days 5, 12, 19, and 26 of the incubation. For soil mineral N analysis, 2 g fresh soil was extracted with 20 ml of 2 M KCl solution (1:10) for 1 h on a reciprocating shaker. The suspensions obtained were centrifuged at 112 ×*g* for 10 min, filtered through a 0.45-μm Syringe Filter PES, and stored at 4 °C for analysis in the next day. The solution would be frozen for storage if the

analysis is not immediately.

The concentrations of INH_4, INO_3, WNH_4, WNO_3, SNH_4, and SNO_3 were measured using an AQ400 Discrete Analyser (SEAL Analytical Ltd., Wrexham, United Kingdom).

2.5. Measurement of additional soil properties

Ten grams of air-dried soil were mixed with 25 ml deionized water (1:2.5) and shaken for 30 min at 200 rpm for pH measurement. The pH of the upper clear liquid was measured using a pH meter (Mettler Toledo, FiveEasy™, FE20). Soil total dissolved organic carbon (TOC) and soil total dissolved nitrogen (TDN) were extracted with 2 M KCl solution (1:10) and measured by TOC-L CPH with ASI-L (Shimadzu, Kyoto, Japan). Soil particle sizes were measured using a Mastersizer 2000 particle analyser (Malvern Panalytical, Malvern, United Kingdom). Soil total carbon (TC) and total nitrogen (TN) were measured using a Flash Smart elemental analyser (Thermo Scientific, Massachusetts, US).

2.6. Statistical analysis

Tukey's honest significant difference (HSD) test was used to compare the means of soil total CO_2-C, N_2O-N, and CH_4-C emissions and soil GWP under different treatments if the treatment effects were significant at the $P < 0.05$ level. Differences for soil initial index (soil properties before experiment) were compared between grassland soil and arable soil under Tukey's HSD test.

Principal component analysis (PCA) were used to test the relation among all GHGs samples. Correlation analysis were used to test the relation between GHGs and soil properties. Variation partitioning were used to found out the contribution of soil properties to GHGs emissions. All statistical analyses were performed using R statistical language (Oakland, CA, USA). PCA and variance decomposition of CO_2-C, N_2O-N, and CH_4-C emissions were computed using the "RDA" and "VARPART" function of the "vegan" library for R (Oksanen and O'Hara, 2005).

3. Results

3.1. Soil moisture changes with time during flooding–drying

Soil moisture decreased with time and decreased to 100% WHC in 10 days under FD (Fig. 2). Soil moisture decreased faster in arable soil than in grassland soil (Fig. 2).

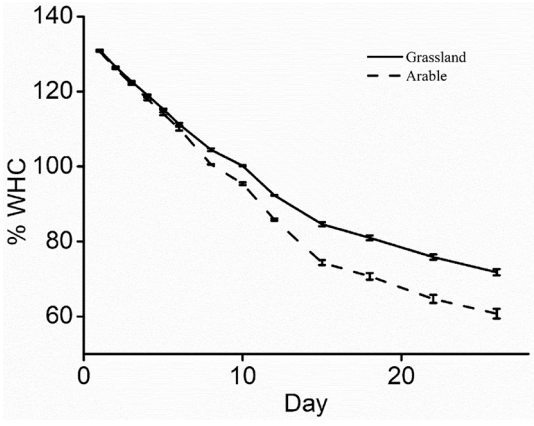

Fig. 2. Soil moisture changes with time under grassland and arable soil during the flooding–drying treatment. The data values are means of three independent pot replicates and error bars represent the standard error of the means ($n = 3$).

3.2. Soil CO_2-C, N_2O-N, and CH_4-C emissions

3.2.1. Rate of CO_2-C, N_2O-N, and CH_4-C emissions

The rate of N_2O-N, CO_2-C, and CH_4-C emissions in grassland and arable soils did not change over time under PF, and that of N_2O-N and CH_4-C emissions in arable soil did not change over time under FD (Fig. 3). The arable soil had a higher rate of N_2O-N emissions than the grassland soil under PF (Fig. 3).

The rate of N_2O-N emissions in grassland soil under FD increased over time, especially after 10 days, when the SM level started to drop below 100% WHC. Arable soil had a higher rate of N_2O-N emissions than grassland soil during the first 15 days under saturated conditions, but decreased when moisture started to fall below 80% WHC (Fig. 3). Thus, arable soil sustained high N_2O emissions under water saturation conditions and grassland enhanced N_2O production following a decline in SM below 80% WHC from Day 15 onwards. The rate of CO_2-C emissions in arable and grassland soil under FD increased over time (Fig. 3). Grassland soil had a higher rate of CO_2-C emissions than arable soil under FD (Fig. 3). The rate of CH_4-C emissions in grassland soil under FD increased and then decreased over time (Fig. 3). Arable soil had a lower rate of CH_4-C emissions than grassland soil under FD (Fig. 3).

3.2.2. Total CO_2-C, N_2O-N, and CH_4-C emissions

The grassland soil under FD had the highest ($P < 0.05$) total N_2O-N, CO_2-C, and CH_4-C emissions (Table 2). The grassland soil under PF had the lowest ($P < 0.05$) total N_2O-N emissions (Table 2). The grassland and arable soil under PF had the lowest ($P < 0.05$) total CO_2-C emissions (Table 2). The arable soil under FD, and the grassland and arable soil under PF had the lowest ($P < 0.05$) total CH_4-C emissions (Table 2).

3.2.3. Global warming potential

Grassland soil had highest ($P < 0.05$) GWP under FD (Table 3). Grassland soil had lowest ($P < 0.05$) GWP under PF (Table 3). Arable soil had a moderate GWP under both PF and FD (Table 3).

3.3. Soil NH_4^+-N and NO_3^--N concentrations

The WNH_4 concentrations of grassland soil decreased and WNO_3 concentrations of grassland increased over time under PF and FD but WNH_4 concentrations decreased rapidly under FD (Fig. 4a). The WNH_4 concentrations of arable soil decreased and WNO_3 concentrations of arable soil rapidly increased with time under PF (Fig. 4a). The WNH_4 concentrations of arable soil decreased rapidly, whereas WNO_3 concentrations increased slightly over time under FD (Fig. 4a).

The INH_4 and INO_3 concentrations of grassland soil and INH_4 concentrations of arable soil were very small and did not change substantially over time under PF and FD (Fig. 4b). The INO_3 concentrations of arable soils did not change over time under PF, and INO_3 concentrations was highest in arable land under PF compared with other soils and treatments (Fig. 4b). The INO_3 concentrations of arable soil under FD decreased in the first 20 incubation days and increased thereafter (Fig. 4b).

The SNH_4 concentrations of grassland decreased and SNO_3 concentrations of grassland were stable over time under PF (Fig. 4c). The SNH_4 concentrations of grassland soil decreased rapidly and SNO_3 concentrations of grassland soil increased slightly over time under FD (Fig. 4c). The SNH_4 concentrations of arable soil decreased slightly and SNO_3 concentrations of arable soil increased slightly over time under PF (Fig. 4c). The SNH_4 concentrations of arable soil decreased rapidly and SNO_3 concentrations of arable soil increased slightly over time under FD (Fig. 4c).

The TDN-N concentrations of grassland soil decreased and TOC-C concentrations of grassland increased over time under PF (Fig. 4d). The TDN-N and TOC-C concentrations of grassland decreased over time under FD (Fig. 4d). The TDN-N concentrations of arable decreased and TOC-C concentrations of arable soil remained stable over time under PF

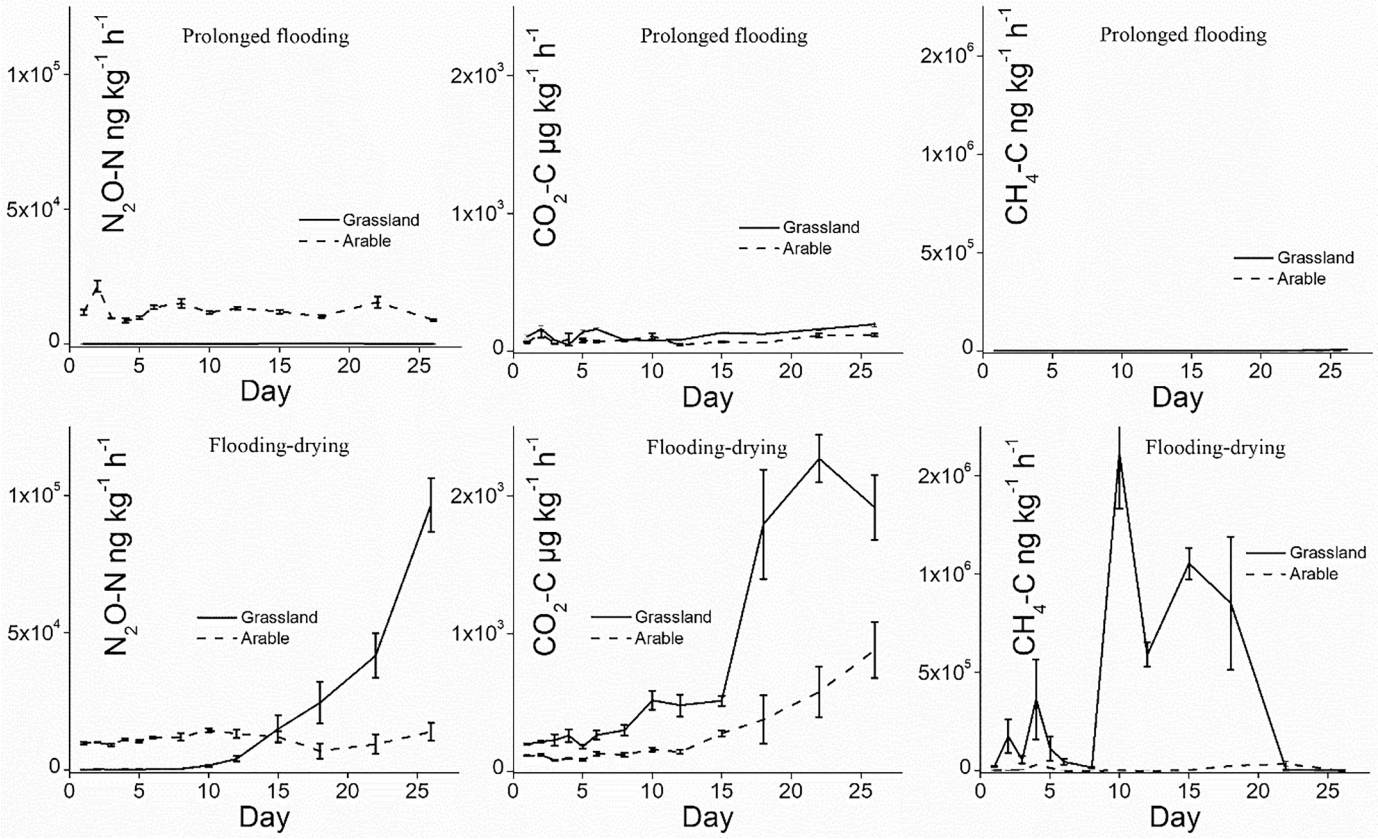

Fig. 3. Rate of soil CO_2-C, N_2O-N, and CH_4-C emissions over time in the grassland and arable soils. The data values are means of three independent pot replicates and error bars represent the standard error of the means ($n = 3$).

Table 2
Soil total CO_2-C, N_2O-N, and CH_4-C emissions. Means of the same gas with the same lower-case letter are not significantly different at the $P < 0.05$ level on the basis of Tukey's HSD test.

	Soil type	N_2O-N mg kg^{-1}	CO_2-C mg kg^{-1}	CH_4-C mg kg^{-1}
Prolonged flooding	Grassland	0.08 (±0.02) a	79.50 (±1.50) a	0.70 (±0.05) a
	Arable	7.82 (±0.21) b	53.72 (±2.82) a	0.02 (±0.01) a
Flooding-drying	Grassland	13.31 (±0.72) c	623.40 (±30.01) c	278.02 (±43.91) b
	Arable	6.89 (±0.76) b	197.89 (±21.91) b	7.26 (±1.24) a

Note: Average value (± relative standard deviation), $n = 3$.

Table 3
Global warming potential. Means with same lower-case letter are not significantly different at the $P < 0.05$ level on the basis of Tukey's HSD test.

GWP (g CO_2 kg^{-1})	Prolonged flooding	Flooding-drying
Grassland	0.39 (±0.02) a	24.02 (±2.25) c
Arable	7.52 (±0.21) b	7.42 (±0.84) b

Note: Average value (± relative standard deviation), $n = 3$.

and FD (Fig. 4d).

3.4. Principal component analysis of soil variation in soil GHG emission

Principal Component 1 (PC1) explained 37.2% of variation in soil GHG emission rates and Principal Component 2 (PC2) explained 26.3% (Fig. 5). Samples of grassland and arable soils with SM > 100% WHC, and grassland and arable soils with SM < 100% WHC were clearly separated from each other (Fig. 5). Grassland and arable soils, with SM > 100% WHC showed a slight relation to soil N_2O-N emissions rate. Grassland and arable soils with SM < 100% WHC had a strong relation to N_2O-N emissions rate, which varied overall and peaked on different days in the two land use types (Fig. 5). The WHC had a strong negative relation to soil N_2O-N emissions rate (increased WHC decreased the soil N_2O-N emissions rate). Soil CO_2-C emissions rate had a strong positive relation to soil N_2O-N emissions rate (Fig. 5).

3.5. Correlation analysis of soil variation in soil GHG emissions

We separated the date between SM > 100% WHC and SM < 100% WHC to conduct the correlation analysis of soil variation since samples of SM > 100% WHC and SM < 100% WHC were clearly separated with each other in the PCA (Fig. 5).

The rate of soil N_2O-N emissions in grassland soils under SM > 100% WHC showed a significant correlation with soil WHC and WNO_3 (Table 4). The rate of soil N_2O-N emissions from grassland soils under SM < 100% WHC had a significant correlation with soil WHC, INH_4, INO_3, and SNO_3 (Table 4).

The rate of soil CO_2-C emissions in grassland soil under SM > 100% WHC showed a significant correlation with INO_3, WNO_3, and TOC-C (Table 4). The rate of soil CO_2-C emissions from grassland soil under SM < 100% WHC showed a significant correlation with SNO_3 and TOC-C (Table 4). The rate of soil CO_2-C emissions in arable soil under SM > 100% WHC showed a significant correlation with INH_4 and INO_3 (Table 4). The rate of soil CO_2-C emissions from arable soil under SM < 100% WHC showed a significant correlation with soil WHC, INH_4, SNH_4, and TDN-N (Table 4). The rate of soil CH_4-C emissions in arable soil

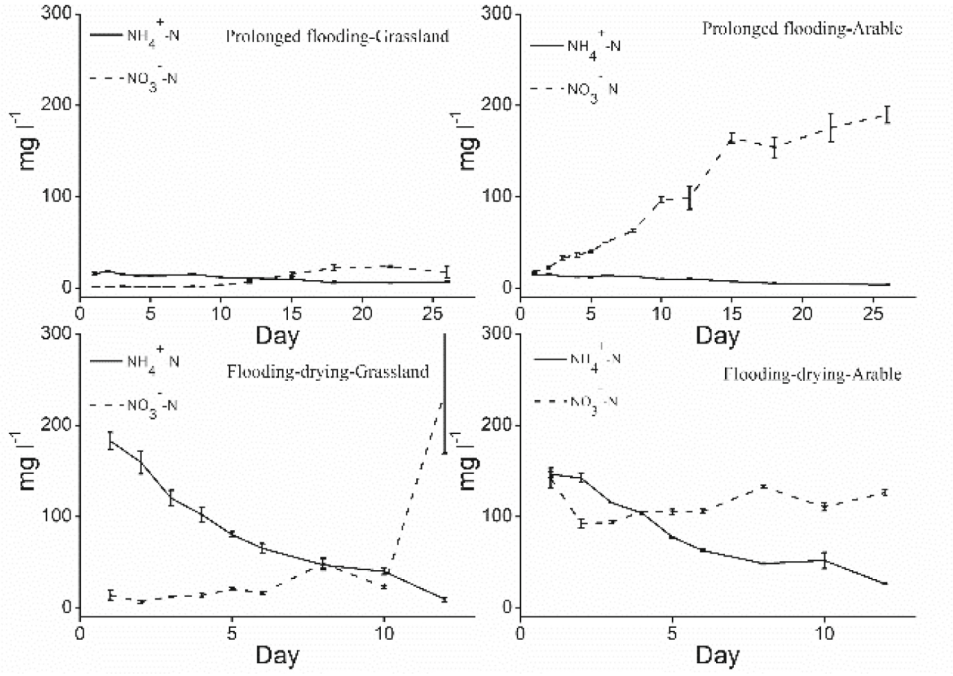

a

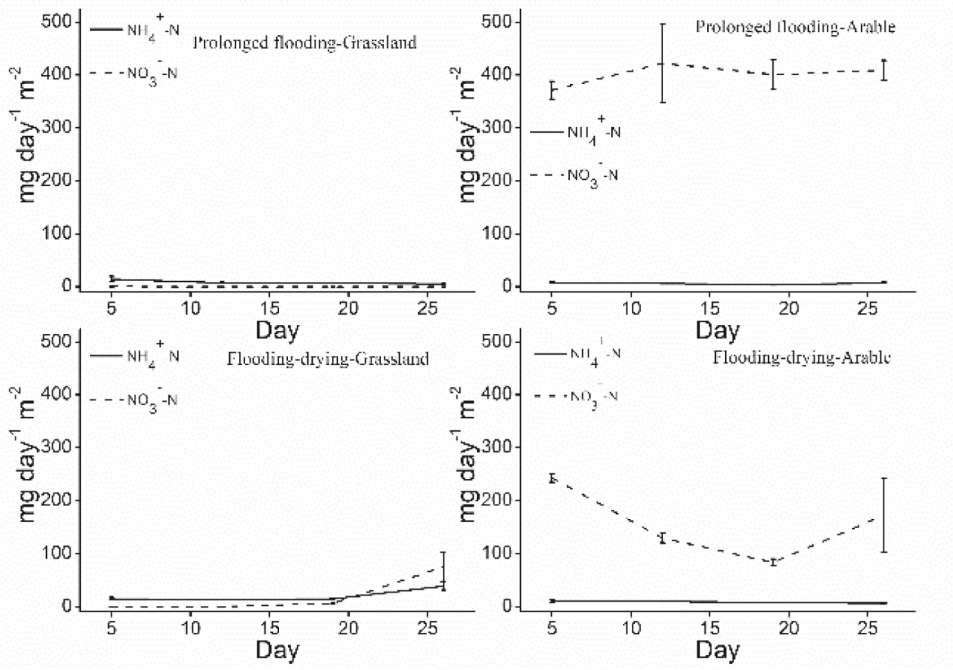

b

Fig. 4. Soil NH_4^+-N and NO_3^--N concentrations from soil pore water (a), ion-exchange resin membranes (b), soil extraction by KCl (c), and extracted total dissolved organic carbon (TOC-C) and total dissolved nitrogen (TDN-N) concentrations (d) over time under grassland and arable land use. The data values are means of three independent pot replicates and error bars represent the standard error of the means ($n = 3$).

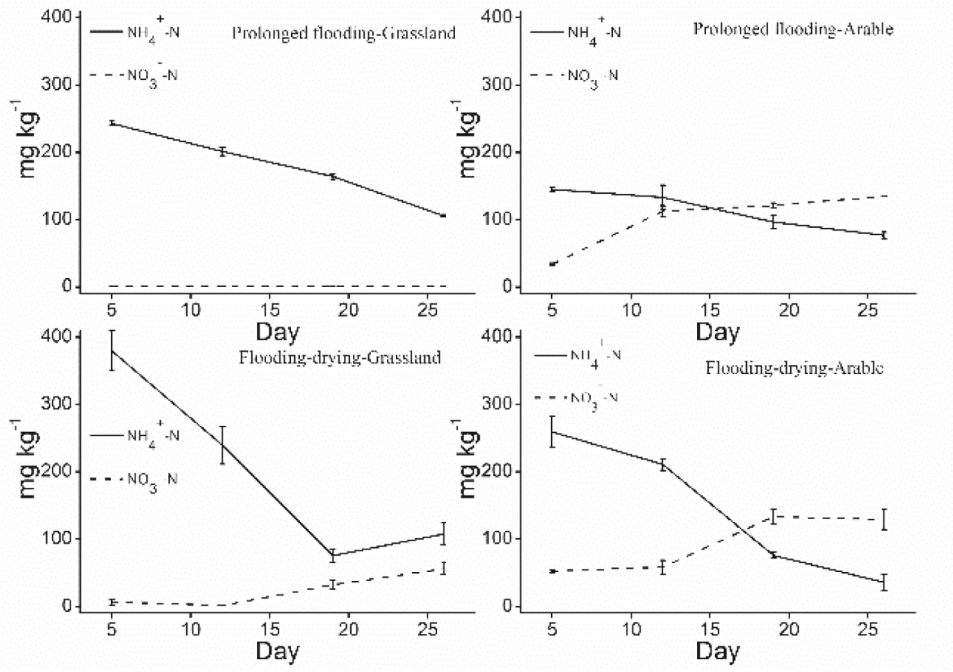

c

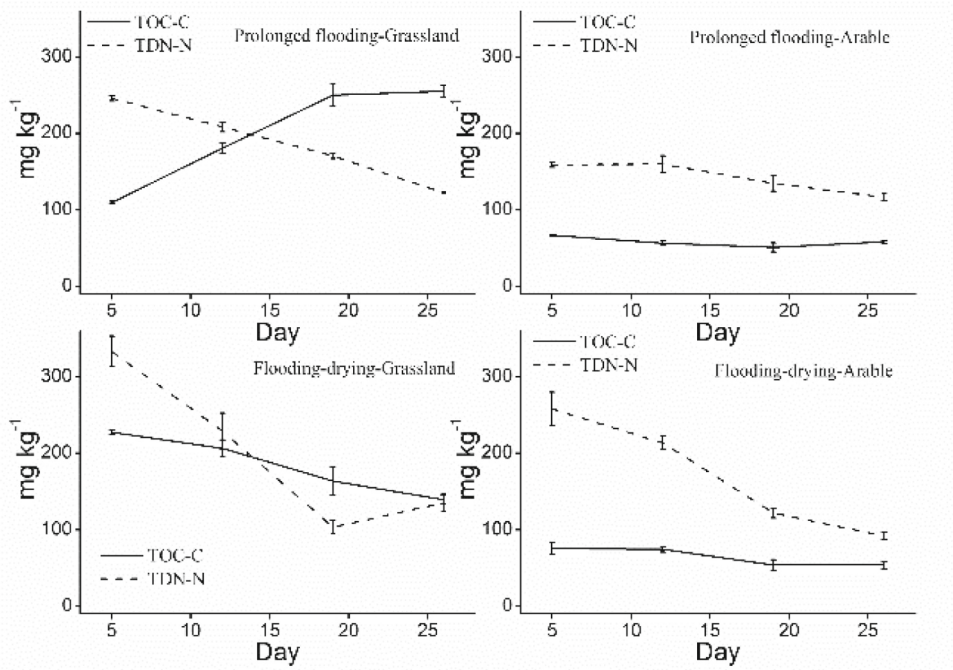

d

Fig. 4. (*continued*).

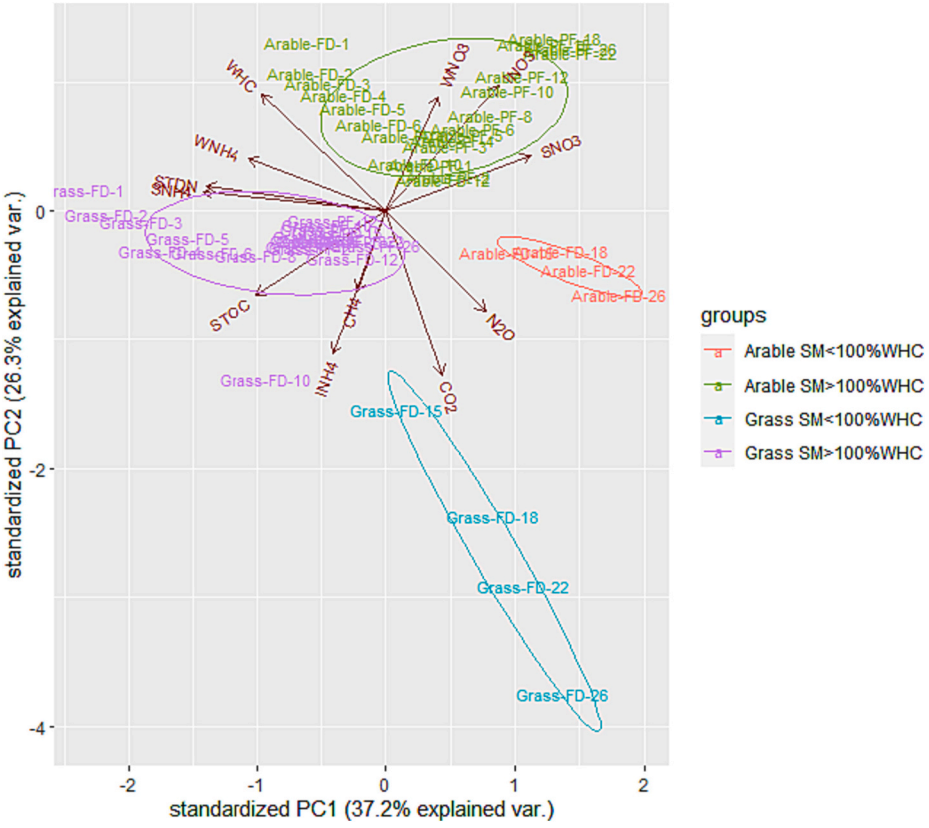

Fig. 5. Principal component analysis of variation in soil GHG emission under grassland and arable soil. N2O, rate of soil N_2O-N emissions; CO2, rate of soil CO_2-C emissions; CH4, rate of soil CH_4-C emissions; WHC, soil water-holding capacity (%); INH4, soil NH_4^+-N concentrations from ion-exchange resin membranes; INO3, soil NO_3^--N concentrations from ion-exchange resin membranes; WNH4, soil NH_4^+-N concentrations from soil pore water; WNO3, soil NO_3^--N concentrations from soil pore water; SNH4, soil NH_4^+-N concentrations from soil extraction by KCl; SNO3, soil NO_3^--N concentrations from soil extraction by KCl; STOC, soil total dissolved organic carbon-carbon; STDN, soil total dissolved nitrogen-nitrogen; SM, soil moisture.

Table 4
Correlation analysis of soil variation in soil GHG emission rates under grassland and arable soil when soil moisture >100% WHC and < 100% WHC. N_2O-N, rate of soil N_2O-N emissions; CO_2-C, rate of soil CO_2-C emissions; CH_4-C, rate of soil CH_4-C emissions; WHC, % of soil water-holding capacity; INH_4, soil NH_4^+-N concentrations from ion-exchange resin membranes; INO_3, soil NO_3^--N concentrations from ion-exchange resin membranes; WNH_4, soil NH_4^+-N concentrations from soil pore water; WNO_3, soil NO_3^--N concentrations from soil pore water; SNH_4, soil NH_4^+-N concentrations from soil extraction by KCl; SNO_3, soil NO_3^--N concentrations from soil extraction by KCl; TOC-C, soil total dissolved organic carbon-carbon; TDN-N, soil total dissolved nitrogen-nitrogen; SM, soil moisture.

Soil type		SM > 100% WHC 1–12 (130)			SM < 100% WHC		
		N_2O-N	CO_2-C	CH_4-C	N_2O-N	CO_2-C	CH_4-C
Grassland	N_2O-N	1.00	0.78**	0.59**	1.00	0.65	−0.73
	CO_2-C	0.78**	1.00	0.81**	0.65	1.00	−0.69
	CH_4-C	0.59**	0.81**	1.00	−0.73	−0.69	1.00
	WHC	−0.59**	−0.36	−0.37	−0.89*	−0.86	0.66
	INH_4	0.01	0.13	0.10	0.97**	0.67	−0.86
	INO_3	−0.39	−0.54**	−0.34	0.97**	0.68	−0.86
	WNH_4	−0.09	0.22	0.07	–	–	–
	WNO_3	0.95**	0.64**	0.32	–	–	–
	SNH_4	−0.02	0.26	0.12	−0.52	−0.86	0.28
	SNO_3	−0.07	0.27	0.07	0.89*	0.89*	−0.69
	TOC-C	0.22	0.43*	0.20	−0.86	−0.91*	0.65
	TDN-N	−0.05	0.21	0.09	−0.47	−0.84	0.23
Arable	N_2O-N	1.00	0.29	−0.17	1.00	0.15	−0.84
	CO_2-C	0.29	1.00	−0.02	0.15	1.00	0.10
	CH_4-C	−0.17	−0.02	1.00	−0.84	0.10	1.00
	WHC	−0.34	−0.31	0.30	0.16	−0.93*	−0.36
	INH_4	−0.14	0.43*	0.41	0.12	−0.96**	−0.33
	INO_3	0.01	−0.61**	−0.32	0.77	0.68	−0.43
	WNH_4	−0.31	0.26	0.52*	–	–	–
	WNO_3	−0.18	0.31	0.07	–	–	–
	SNH_4	−0.21	0.34	0.51*	0.32	−0.88*	−0.47
	SNO_3	−0.09	0.00	−0.10	−0.53	0.74	0.60
	TOC-C	−0.09	0.39	0.38	0.50	−0.77	−0.58
	TDN-N	−0.24	0.34	0.53*	0.31	−0.89*	−0.46

* Significant at $P < 0.05$.
** Significant at $P < 0.01$.

under SM > 100% WHC showed a significant correlation with WNH_4, SNH_4, and TDN-N (Table 4).

3.6. Variation partitioning of soil N_2O-N emissions

WHC and WNO_3 were selected to conduct the variation partitioning of N_2O-N emissions when SM > 100% WHC in grassland soil, since WHC and WNO_3 showed a significant correlation with soil N_2O-N emissions (Table 4). WHC, INH_4, INO_3, and SNO_3 were selected to conduct the variation partitioning of N_2O-N emissions when SM < 100% WHC in grassland soil since WHC, INH_4, INO_3, and SNO_3 showed a significant correlation with soil N_2O-N emissions (Table 4).

WNO_3 of grassland soil had the highest contribution to N_2O-N emissions (58%) when SM > 100% WHC (Fig. 6a). The combined effect of SNO_3 and INH_4 had the highest contribution to N_2O-N emissions (71%) when SM < 100% WHC in grassland soil (Fig. 6b).

4. Discussion

4.1. The GHG emissions and NH_4^+-N and NO_3^--N dynamics under prolonged flooding

The SNH_4 of grassland and arable decreased and SNO_3 of grassland and arable soils remained stable or increased slightly over time under PF, whereas the WNH_4 of grassland and arable soils deceased and WNO3 of grassland and arable soils increased over time under PF (Fig. 4). This could be because small amounts of NH_4^+-N that were absorbed by soil particles (stable) were slowly released to soil pore water (available). The available NH_4^+-N and TDN-N seem to have been key substrates for nitrification (NO_3^--N production) in our grassland and arable soil. The dynamics of SNH_4, SNO_3, and WNO_3 concentration combined with the lower N_2O emissions and GWP under PF (Fig. 3 and Table 3) showed that small amounts of NO_3^--N were denitrified to N_2O-N and most of the NO_3^--N was denitrified to N_2 under the 110% WHC conditions of PF. This supports the finding of Wu et al. (2017) that excessive moisture condition can suppress N_2O emissions through its reduction to N_2 during complete denitrification. Previous studies have reported low N_2O emissions from flooded fields (Shaaban et al., 2018; Song et al., 2021; Xu et al., 2022), which is commensurate with our finding that PF had lower N_2O emissions than FD. Flooding generally induce soil anaerobic conditions, consequently limiting mineralization of organic C and N, and ultimately resulting in less substrates for N_2O production via nitrification and denitrification (Li et al., 2022; Neubauer and Megonigal, 2021). These conditions are favourable for complete denitrification producing N_2 rather than N_2O, and therefore low N_2O emissions (Cai et al., 2013; Mazza et al., 2018). Moreover, the decrease in N_2O emissions during continuously flooded soil can also rapidly deplete and entrap NO_3^- within the micropores, possibly limiting further denitrification to produce N_2O and N_2 gases (McNicol and Silver, 2014).

Arable soil had a higher rate of N_2O-N emissions than grassland soil under PF (Fig. 3), and the arable soil had significantly higher total N_2O-N emissions and GWP than grassland soil under PF (Tables 2 and 3) with a higher INO_3 concentration (Fig. 4b) and decomposition of TDN-N (Fig. 4d). This could be because arable soil had a smaller pH compared with grassland soil and arable soil had more nitrate compared with grassland soil from the beginning (Table 1). Ćuhel et al. (2010) found that the relative importance of N_2O as a product of denitrification is higher at low pH. The functionality of the *nosZ* gene for synthesizing N_2O-reducing enzyme (N_2O reductase) is limited under low pH, leading to higher N_2O emissions (Shaaban et al., 2018). High soil pH values also typically shift the denitrification end product ratio towards N_2 instead of N_2O (Šimek et al., 2002) and lower N_2O formation during nitrification (Mørkved et al., 2007). Bell et al. (2015) also found that the annual emissions factor for a Scottish arable soil was 3–5 times higher than grassland sites elsewhere in the UK, which supports our findings of greater N_2O-N emissions from arable than grassland soil.

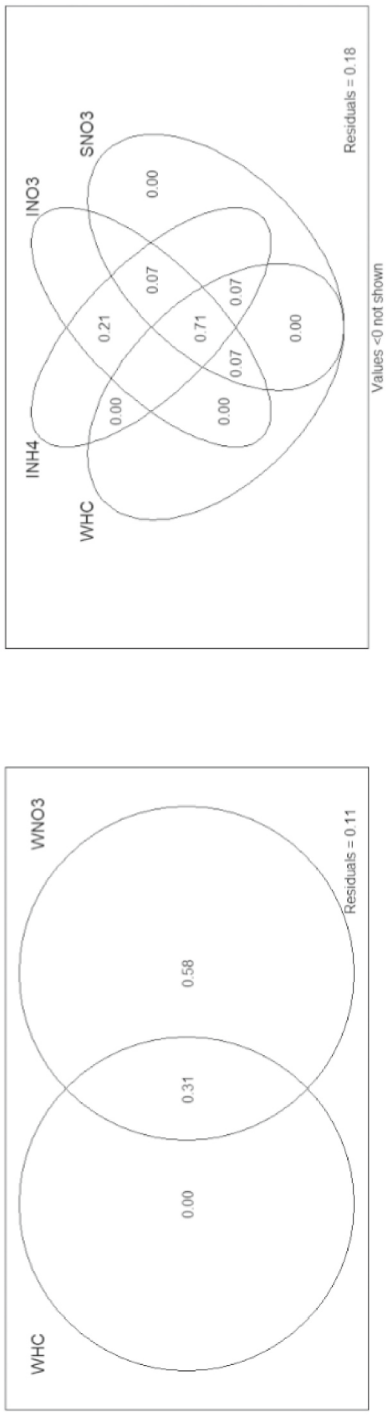

Fig. 6. Variation partitioning of N_2O-N emissions for soil moisture exceeding 100% water-holding capacity (a) and soil moisture lower than 100% water-holding capacity (b) in grassland soil. WHC, soil water-holding capacity (%); INH4, soil NH_4^+-N concentrations from ion-exchange resin membranes; INO3, soil NO_3^--N concentrations from ion-exchange resin membranes; WNO3, soil NO_3^--N concentrations from soil pore water; SNO3, soil NO_3^--N concentrations from soil extraction by KCl.

The CO_2 and CH_4 emissions were low in both grassland and arable soil under PF (Fig. 3 and Table 2). This is likely to be because the high-water content limited the decomposition of soil organic matter and dissolved the CH_4. Devüvre and Horwáth (2000) and Khalid et al. (2019) showed that mineralization of SOC was restrained under waterlogged conditions by restricting microbial growth and activities, and thereby impeded CO_2 production. The unexpected low CH_4 emissions seem to have resulted from low diffusion into air under flooding/saturated soils conditions. Moreover, under saturated conditions, interaction of methanogens and nitrate reducers, which utilize acetate and H_2 more efficiently than methanogens may have further reduced potential CH_4 fluxes (Conrad, 2002) for arable soil. Another possible explanation for the low CH_4 emission might be the use of ammonium sulphate as fertilizer, where ammonium competitively inhibits methanography (Ullah et al., 2008) in rice fields (Linquist et al., 2012).

4.2. The GHG emissions and NH_4^+-N and NO_3^--N dynamic under flooding–drying

The WNH_4 of grassland and arable soils decreased and WNO_3 of grassland and arable soils increased over time under FD, while the SNH_4 of grassland and arable soils strongly decreased and SNO_3 of grassland and arable increased slightly over time under FD (Fig. 4c). When SM > 100% WHC, lower N_2O emissions were detected under FD in grassland and arable soils (Fig. 3). This is similar to the findings for PD described in Section 4.1. When SM < 100% WHC, N_2O-N emissions were high under FD in grassland soil and N_2O-N emissions increased as SM decreased (Fig. 3). This was mainly because nitrification-denitrification and denitrification increased over time in grassland soil. Freibauer et al. (2004) and Goldberg et al. (2010) also found that degradation of soil organic matter as a result of drainage and cultivation will stimulate net N mineralization and N transformations via nitrification and denitrification, leading to N_2O production. The soil pore structure is important for GHG production and diffusion at the soil-air interface. At the capillary fringe above the water level, the soil is characterized by having close to sub-saturated SM and mixed aerobic and anaerobic conditions, promoting the environmental conditions favourable for both N_2O production via denitrification and NO_3^- reduction via DNRA (Megonigal et al., 2003). Several researchers (Congreves et al., 2019; Miller et al., 2020) have found that the products of N_2O by denitrification increase with decreasing water-filled pore space from 90% to 60%. Moreover, the N_2O products peaked at optimum water filled pore space of 65%–70% (Pärn et al., 2018; van Lent et al., 2015; Werner et al., 2007). Denitrification becomes more prevalent at higher water contents, leading to maximum emissions at around 80% WHC (Shepherd, 2009). In agricultural soils, the total N_2O emissions in a season are strongly related to the episodes of large N_2O pulses observed after irrigation and rainfall events, which are primarily derived from denitrification (Trost et al., 2013). This is consistent with our finding that N_2O-N emissions increased with the decrease of SM towards the end of the experiment (SM was still higher than 60% WHC).

The TDN-N and TOC-C of grassland decreased with time under FD (Fig. 4d). However, TDN-N decreased but TOC-C remained stable with time in arable soils under FD (Fig. 4d). Arable soil also had a lower N_2O-N emissions rate than grassland soil when SM was below 80% WHC under FD (Fig. 3) and the grassland soil had higher total N_2O-N emissions and GWP than arable soil under FD (Tables 3 and 4). This could be because soil N, C, and microbes in arable soil limited the nitrification and denitrification, and therefore lowered the production of N_2O-N under SM < 100% WHC. The C-substrate availability and N_2O emissions from denitrification and nitrification are always positively related to each other (Li et al., 2005; Wan et al., 2009) because nitrification is primarily an autotrophic process and heterotrophic nitrification only accounts for 20% or less under low-pH conditions (Liu et al., 2015). Gütlein et al. (2018) also found that N_2O emissions correlated positively with SM and total soil nitrogen content. Short and temporary drying-rewetting frequency enhanced denitrifier activity by availing physically protected organic matter (Fierer and Schimel, 2002). The N_2O derived from soil organic matter decomposition dominates overall fluxes (Maljanen et al., 2010). Abbasi et al. (2011) also found that the process of denitrification and production of N_2O was smaller in arable soil deficient in organic matter compared with grassland soil because of the lower availability of organic C. Another reason is that grassland soil has a higher pH (Table 1), which then leads to higher N_2O-N emissions when SM < 100% WHC (Fig. 3 and Table 2). Fan et al. (2018) reported significantly higher N_2O emissions rates from three alkaline soils (pH 7.6–8.2) as compared with an acidic soil with a pH of 5.6. Oxidation of NH_4^+ is completely inhibited at pH 5 but increases as pH increases (Wang et al., 2018) through a pH-driven shift in the microbial community structure and/or microbial activities (Ottosen et al., 2009).

The soil TC and TOC were mainly anaerobically digested to CH_4 before 15 days (especially when SM was between 110% and 80%) and aerobically digested to CO_2 after 15 days in FD grassland soil when SM was lower than 80% WHC (Fig. 3). Methane production is expected to mainly occur below the groundwater table (Segers, 1998). Anaerobic conditions during the flooding stage of the experiment promoted methanogenic activities while suppressing methanotrophic activities, leading to CH_4 production (Shaaban et al., 2022). Drainage will limit the production of CH_4 because the highest oxidation potentials are found near the oxic–anoxic interface (Petersen et al., 2012). However, draining can also increase the potential for CH_4 oxidation during passage through the unsaturated zone to the atmosphere (Petersen et al., 2012). In general, CO_2 fluxes are dominant at drained sites (Kandel et al., 2018) and show a decreasing trend following an increase of soil water content (Smith et al., 2003; McNicol and Silver, 2014). This is because of a lower O_2 availability and the consequent inhibition of aerobic respiration when a large proportion of pores are saturated under flooding (Mazza et al., 2018). Khalid et al. (2019) showed that CO_2 emissions were significantly larger in a flooded soil converted to wet soil treatment compared with continuously flooded and wet soil treatments, which they suggested was due to increased mineralization and C contents. In our study, the CH_4 emissions after 100% WHC (Fig. 3) may be due to the gas entrapment into microaggregates and a delayed release (either as emissions or leaching) (Mazza et al., 2018). The CH_4 emissions increased during the second flooding event (FD) relative to the first (PF) (Fig. 3), which could relate to some mechanism of adaptation by microbial communities (Lagomarsino et al., 2016).

The grassland soil had a higher rate of CO_2-C and CH_4-C emissions than the arable soil under FD (Fig. 3). The grassland soil under FD had significantly higher total CO_2-C and CH_4-C emissions and GWP than arable soil (Tables 3 and 4). The organic matter and TN contents were higher in grassland soils than in arable soils (Table 1), leading to higher potential for mineralization after disturbance (drainage) (Eickenscheidt et al., 2014). Volpi et al. (2017) found that CO_2 emissions are positively linked to SOC content and denitrification activity, which also increases CO_2 efflux (Groffman and Crawford, 2003). Therefore, grassland soil under FD had significantly higher total CO_2-C and CH_4-C emissions and GWP than arable soil under FD. Thomson et al. (2010) detected significantly higher respiration rates in dried and rewetted microcosms. When the SM content decreased from flooded to 60% WFPS, CH_4 emissions decreased, but N_2O and CO_2 emissions substantially increased because the flooded soil released N and C and triggered C and N cycling (Shaaban et al., 2022). We similarly found higher GHG emissions and GWP under FD than PF in grassland soil (Tables 2 and 3).

4.3. The influence of different types on soil NH_4^+-N and NO_3^--N contents on GHG emissions

Grassland and arable soil sample of N_2O-N emissions were clearly separate between SM > 100% WHC and SM < 100% WHC (Fig. 5). Senbayram et al. (2009) found that the high NO_3^- availability as a result of nitrification, together with labile C under anaerobic soil conditions,

serves as a driving force for N_2O emissions. We also found that the N_2O-N and CO_2-C emissions were mainly controlled by soil available NO_3^--N when SM exceeded 100% WHC, whereas N_2O-N emissions were controlled by soil stable NH_4^+-N and NO_3^--N when SM was lower than 100% WHC in the grassland soil (Fig. 6).

5. Conclusion

Changes in soil moisture as influenced by PF and FD as proxies of climate change significantly affected the GHG flux of arable and grassland soils differently. Higher N_2O-N, CO_2-C, and CH_4-C emissions and large GWP were found in grassland soil under FD, and these fluxes were mainly controlled by soil NH_4^+-N, NO_3^--N, and TOC concentrations when soil moisture was lower than 100% WHC. Arable soils exhibited similar GWP both under PF and FD. Compared to grassland, arable soil had higher GWP than grassland soils under PF, which switched significantly under FD where the GWP of grassland soils was order of magnitude higher than arable soils. Future climate change will most likely result in intense precipitation resulting in soils saturation followed by drying and under such conditions, temperate grasslands will emit more GHG than arable soils. This suggests that land use conversion and/or rotations from arable to grassland soils for improving soil health or carbon sequestration shall consider the changing source-strength of GHG fluxes in the overall carbon and GHG budgets under national GHG and carbon sequestration inventories and the net zero GHG ambitions. Repeating this experiment in the field with undisturbed soil samples will carry out for further study.

Declaration of Competing Interest

The authors declare that they have no known competing financial interests or personal relationships that could have appeared to influence the work reported in this paper.

Data availability

Data will be made available on request.

Acknowledgements

This research was supported by the UKRI-NERC under the joint project “Signals in the Soils”. Large Area Distributed Real Time Soil (DiRTS) Monitoring and BBSRC (BB/R021716/1). The authors would like to thank Gianni Micucci (PhD student) for support in field campaigns, James Gore (Research Technician) for laboratory training, and Andrea Rabbai, Manon Rumeau, Thanawan Buacharoen, Jessica Chadwick (PhD students) and Johanna Pihlbald (Research Fellow) for help in laboratory work and instrumental analysis.

References

Abbasi, M.K., Hina, M., Tahir, M.M., 2011. Effect of *Azadirachta indica* (neem), sodium thiosulphate and calcium chloride on changes in nitrogen transformations and inhibition of nitrification in soil incubated under laboratory conditions. Chemosphere 82, 1629–1635. https://doi.org/10.1016/j.chemosphere.2010.11.044.

Bell, M.J., Hinton, N., Cloy, J.M., Topp, C.F.E., Rees, R.M., Cardenas, L., Scott, T., Webster, C., Ashton, R.W., Whitmore, A.P., Williams, J.R., Balshaw, H., Paine, F., Goulding, K.W.T., Chadwick, D.R., 2015. Nitrous oxide emissions from fertilised UK arable soils: fluxes, emission factors and mitigation. Agric. Ecosyst. Environ. 212, 134–147. https://doi.org/10.1016/j.agee.2015.07.003.

Cai, Y., Ding, W., Luo, J., 2013. Nitrous oxide emissions from Chinese maize–wheat rotation systems: a 3-year field measurement. Atmos. Environ. 65, 112–122. https://doi.org/10.1016/j.atmosenv.2012.10.038.

Carneiro, J., Cardenas, L.M., Hatch, D.J., Trindade, H., Scholefield, D., Clegg, C.D., Hobbs, P., 2010. Effect of the nitrification inhibitor dicyandiamide on microbial communities and N_2O from an arable soil fertilized with ammonium sulphate. Environ. Chem. Lett. 8, 237–246. https://doi.org/10.1007/s10311-009-0212-3.

Caroline, B., Reinhard, W., Mirjam, H., Roland, F., Manfred, K., Andreas, G., Matthias, B., Heinz, F., 2017. Soil mineral N dynamics and N_2O emissions following grassland renewal. Agric. Ecosyst. Environ. 246, 325–342. https://doi.org/10.1016/j.agee.2017.06.013.

Chen, D.L., Suter, H.C., Islam, A., Edis, R., Freney, J.R., Walker, C.N., 2008. Prospects of improving efficiency of fertiliser nitrogen in Australian agriculture; a review of enhanced efficiency fertilisers. Aust. J. Soil Res. 46, 289–301. https://doi.org/10.1071/SR07197.

Congreves, K.A., Phan, T., Farrell, R.E., 2019. A new look at an old concept: using $^{15}N_2O$ isotopomers to understand the relationship between soil moisture and N_2O production pathways. Soil 5, 265–274. https://doi.org/10.5194/soil-5-265-2019.

Conrad, R., 2002. Control of microbial methane production in wetland rice fields. Nutr. Cycl. Agroecosyst. 64, 59–69. https://doi.org/10.1023/A:1021178713988.

Conrad, R., 2009. The global methane cycle: recent advances in understanding the microbial processes involved: global methane cycle. Environ. Microbiol. Rep. 1, 285–292. https://doi.org/10.1111/j.1758-2229.2009.00038.x.

Cranfield soil and agrifood institute, 2023. https://www.landis.org.uk/soilscapes/index.cfm?panel=search#, 2023.

Čuhel, J., Šimek, M., Laughlin, R.J., Bru, D., Chèneby, D., Watson, C.J., Philippot, L., 2010. Insights into the effect of soil pH on N_2O and N_2 emissions and denitrifier community size and activity. Appl. Environ. Microbiol. 76, 1870–1878. https://doi.org/10.1128/AEM.02484-09.

Devüvre, O.C., Horwáth, W.R., 2000. Decomposition of rice straw and microbial carbon use efficiency under different soil temperatures and moistures. Soil Biol. Biochem. 32, 1773–1785. https://doi.org/10.1016/S0038-0717(00)00096-1.

Eickenscheidt, T., Heinichen, J., Augustin, J., Freibauer, A., Drösler, M., 2014. Nitrogen mineralization and gaseous nitrogen losses from waterlogged and drained organic soils in a black alder (*Alnus glutinosa* (L.) Gaertn.) forest. Biogeosciences 11, 2961–2976. https://doi.org/10.5194/bg-11-2961-2014.

Fan, C., Li, B., Xiong, Z., 2018. Nitrification inhibitors mitigated reactive gaseous nitrogen intensity in intensive vegetable soils from China. Sci. Total Environ. 612, 480–489. https://doi.org/10.1016/j.scitotenv.2017.08.159.

Fay, P.A., Kaufman, D.M., Nippert, J.B., Carlisle, J.D., Harper, C.W., 2010. Changes in grassland ecosystem function due to extreme rainfall events: implications for responses to climate change. Glob. Chang. Biol. 14, 1600–1608. https://doi.org/10.1111/j.1365-2486.2008.01605.x.

Fierer, N., Schimel, J.P., 2002. Effects of drying-rewetting frequency on soil carbon and nitrogen transformations. Soil Biol. Biochem. 34, 777–787. https://doi.org/10.1016/S0038-0717(02)00007-X.

Fixon, P.E., West, F.B., 2002. Nitrogen fertilizers: meeting contemporary challenges. AMBIO J. Hum. Environ. 31, 169–176. https://doi.org/10.1579/0044-7447-31.2.169.

Freibauer, A., Rounsevell, M.D.A., Smith, P., Verhagen, J., 2004. Carbon sequestration in the agricultural soils of Europe. Geoderma 122, 1–23, 2004. https://doi.org/10.1016/j.geoderma.2004.01.021.

Gilsanz, C., Báez, D., Misselbrook, T.H., Dhanoa, M.S., Cárdenas, L.M., 2016. Development of emission factors and efficiency of two nitrification inhibitors, DCD and DMPP. Agric. Ecosyst. Environ. 216, 1–8. https://doi.org/10.1016/j.agee.2015.09.030.

Goldberg, S.D., Knorr, K.-H., Blodau, C., Lischeid, G., Gebauer, G., 2010. Impact of altering the water table height of an acidic fen on N_2O and NO fluxes and soil concentrations. Glob. Chang. Biol. 16, 220–233. https://doi.org/10.1111/j.1365-2486.2009.02015.x.

Groffman, P.M., Crawford, M.K., 2003. Denitrification potential in urban riparian zones. J. Environ. Qual. 32, 1144–1149. https://doi.org/10.2134/jeq2003.1144.

Guo, Y.F., Liang, A.Z., Zhang, Y., Zhang, S., Chen, X., Jia, S., Zhang, X., Wu, D., 2019. Evaluating the contributions of earthworms to soil organic carbon decomposition under different tillage practices combined with straw additions. Ecol. Indic. 105, 516–524. https://doi.org/10.1016/j.ecolind.2018.04.046.

Guo, Y.F., Naeem, A., Mühling, K.H., 2021a. Comparative effectiveness of four nitrification inhibitors for mitigating carbon dioxide and nitrous oxide emissions from three different textured soils. Nitrogen 2, 155–166. https://doi.org/10.3390/nitrogen2020011.

Guo, Y.F., Anjum, A., Khan, A., Naeem, A., Mühling, K.H., 2021b. Comparative effectiveness of biogas residue acidification and nitrification inhibitors in mitigating CO_2 and N_2O emissions from biogas residue amended soils. Water Air Soil Pollut. 232, 345. https://doi.org/10.1007/s11270-021-05282-1.

Guo, Y.F., Becker-Fazekas, S., Mühling, K.H., 2022a. Impact of different chloride salts and their concentrations on nitrification and trace gas emissions from a sandy soil under a controlled environment. Soil Use Manag. 38, 861–872. https://doi.org/10.1111/sum.12713.

Guo, Y.F., Naeem, A., Becker-Fazekas, S., Pitann, B., Mühling, K.H., 2022b. Efficacy of four nitrification inhibitors for the mitigation of nitrous oxide emissions under different soil temperature and moisture. J. Plant Nutr. Soil Sci. 185, 60–68. https://doi.org/10.1002/jpln.202000367.

Gütlein, A., Gerschlauer, F., Kikoti, I., Kiese, R., 2018. Impacts of climate and land use on N_2O and CH_4 fluxes from tropical ecosystems in the Mt. Kilimanjaro region, Tanzania. Glob. Chang. Biol. 24, 1239–1255. https://doi.org/10.1111/gcb.13944.

Harter, J., Krause, H.M., Schuettler, S., Ruser, R., Fromme, M., Scholten, T., Kappler, A., Behrens, S., 2014. Linking N_2O emissions from biochar-amended soil to the structure and function of the N-cycling microbial community. ISME J. 8, 660–674. https://doi.org/10.1038/ismej.2013.160.

Hawthorne, I., Johnson, M.S., Jassal, R.S., Black, T.A., Grant, N.J., Smukler, S.M., 2017. Application of biochar and nitrogen influences fluxes of CO_2, CH_4 and N_2O in a forest soil. J. Environ. Manag. 192, 203–214. https://doi.org/10.1016/j.jenvman.2016.12.066.

Hu, H.W., Chen, D., He, J.Z., 2015. Microbial regulation of terrestrial nitrous oxide formation: understanding the biological pathways for prediction of emission rates. FEMS Microbiol. Rev. 39 (5), 729–749. https://doi.org/10.1093/femsre/fuv021.
IPCC, 2001. Climate Change 2001: The Scientific Basis. Cambridge University Press.
IPCC, 2007. Climate Change 2007: The Physical Science Basis. Cambridge University Press.
IPCC, 2021. Climate Change 2021: The Physical Science Basis. Cambridge University Press.
IPCC, 2022. Global Warming of 1.5°C: IPCC Special Report on Impacts of Global Warming of 1.5°C above Pre-Industrial Levels in Context of Strengthening Response to Climate Change, Sustainable Development, and Efforts to Eradicate Poverty. Cambridge University Press. https://doi.org/10.1017/9781009157940.
Jørgensen, C.J., Elberling, B., 2012. Effects of flooding-induced N_2O production, consumption and emission dynamics on the annual N_2O emission budget in wetland soil. Soil Biol. Biochem. 53, 9–17. https://doi.org/10.1016/j.soilbio.2012.05.005.
Kandel, T.P., Lærke, P.E., Elsgaard, L., 2018. Annual emissions of CO_2, CH_4 and N_2O from a temperate peat bog: comparison of an undrained and four drained sites under permanent grass and arable crop rotations with cereals and potato. Agric. For. Meteorol. 256-257, 470–481. https://doi.org/10.1016/j.agrformet.2018.03.021.
Khalid, M.S., Shaaban, M., Hu, R., 2019. N_2O, CH_4, and CO_2 emissions from continuous flooded, wet, and flooded converted to wet soils. J. Soil Sci. Plant Nutr. 19, 342–351. https://doi.org/10.1007/s42729-019-00034-x.
Köster, J.R., Well, R., Dittert, K., Giesemann, A., LewickaSzczebak, D., Mühling, K.H., Herrmann, A., Lammel, J., Senbayram, M., 2013. Soil denitrification potential and its influence on the N_2O reduction and N_2O isotopomer ratios. Rapid Commun. Mass Spectrom. 27, 2363–2373. https://doi.org/10.1002/rcm.6699.
Lagomarsino, A., Agnelli, A.E., Pastorelli, R., Pallara, G., Rasse, D.P., Silvennoinen, H., 2016. Past water management affected GHG production and microbial community pattern in Italian rice paddy soils. Soil Biol. Biochem. 93, 17–27. https://doi.org/10.1016/j.soilbio.2015.10.016.
Li, C., Frolking, S., Butterbach-Bahl, K., 2005. Carbon sequestration in arable soils is likely to increase nitrous oxide emissions, offsetting reductions in climate radiative forcing. Clim. Chang. 72, 321–338. https://doi.org/10.1007/s10584-005-6791-5.
Li, Z., Tang, Z., Song, Z., Chen, W., Tian, D., Tang, S., Wang, X., Wang, J., Liu, W., Wang, Y., Li, J., Jiang, L., Luo, Y., Niu, S., 2022. Variations and controlling factors of soil denitrification rate. Glob. Chang. Biol. 28, 2133–2145. https://doi.org/10.1111/gcb.16066.
Linquist, B.A., Adviento-Borbe, M.A., Pittelkow, C.M., van Kessel, C., van Groenigen, K. J., 2012. Fertilizer management practices and greenhouse gas emissions from rice systems: a quantitative review and analysis. Field Crop Res. 135, 10–21. https://doi.org/10.1016/j.fcr.2012.06.007.
Liu, R., Suter, H., Hayden, H., He, J., Chen, D., 2015. Nitrate production is mainly heterotrophic in an acid dairy soil with high organic content in Australia. Biol. Fertil. Soils 51, 891–896. https://doi.org/10.1007/s00374-015-1026-z.
Liu, Y., Tang, H., Muhammad, A., Huang, G., 2019. Emission mechanism and reduction countermeasures of agricultural greenhouse gases – a review. Greenh. Gases: Sci. Technol. 9, 160–174. https://doi.org/10.1002/ghg.1848.
Malik, A.A., Puissant, J., Buckeridge, K.M., Goodall, T., Jehmlich, N., Chowdhury, S., Gweon, H.S., Peyton, J.M., Mason, K.E., van Agtmaal, M., Blaud, A., Clark, I.M., Whitaker, J., Pywell, R.F., Ostle, N., Gleixner, G., Griffiths, R.I., 2018. Land use driven change in soil pH affects microbial carbon cycling processes. Nat. Commun. 9, 3591. https://doi.org/10.1038/s41467-018-05980-1.
Maljanen, M., Sigurdsson, B.D., Guðmundsson, J., Óskarsson, H., Huttunen, J.T., Martikainen, P.J., 2010. Greenhouse gas balances of managed peatlands in the Nordic countries – present knowledge and gaps. Biogeosciences 7, 2711–2738. https://doi.org/10.5194/bg7-2711-2010.
Mazza, G., Agnelli, A.E., Andrenelli, M.C., Lagomarsino, A., 2018. Effects of water content and N addition on potential greenhouse gas production from two differently textured soils under laboratory conditions. Arch. Agron. Soil Sci. 64, 654–667. https://doi.org/10.1080/03650340.2017.1373184.
McNicol, G., Silver, W.L., 2014. Separate effects of flooding and anaerobiosis on soil greenhouse gas emissions and redox sensitive biogeochemistry. JGR Biogeosci. 119, 557–566. https://doi.org/10.1002/2013JG002433.
Megonigal, J.P., Hines, M.E., Visscher, P.T., 2003. Anaerobic metabolism: linkages to trace gases and aerobic processes. In: Treatise on Geochemistry, 8, pp. 317–424. https://doi.org/10.1016/B0-08-043751-6/08132-9.
Miller, G.A., Rees, R.M., Griffiths, B.S., Cloy, J.M., 2020. Isolating the effect of soil properties on agricultural soil greenhouse gas emissions under controlled conditions. Soil Use Manag. 36, 285–298. https://doi.org/10.1111/sum.12552.
Mørkved, P.T., Dörsch, P., Bakken, L.R., 2007. The N_2O product ratio of nitrification and its dependence on long-term changes in soil pH. Soil Biol. Biochem. 39, 2048–2057. https://doi.org/10.1016/j.soilbio.2007.03.006.
Neubauer, S.C., Megonigal, J.P., 2021. Biogeochemistry of wetland carbon preservation and flux. Wetland carbon and environmental management. In: Geophysical Monograph Series. https://doi.org/10.1002/9781119639305.ch3.
Oksanen, K.J.R., O'Hara, R.B., 2005. Vegan: community ecology package. In: R Package Version 1, pp. 6–9.
Ottosen, L.D.M., Poulsen, H.V., Nielsen, D.A., Finster, K., Nielsen, L.P., Revsbech, N.P., 2009. Observations on microbial activity in acidified pig slurry. Biosyst. Eng. 102 (3), 291–297. https://doi.org/10.1016/j.biosystemseng.2008.12.003.
Park, S., Croteau, P., Boering, K.A., Etheridge, D.M., Ferretti, D., Fraser, P.J., Kim, K.R., Krummel, P.B., Langenfelds, R.L., van Ommen, T.D., Steele, L.P., Trudinger, C.M., 2012. Trends and seasonal cycles in the isotopic composition of nitrous oxide since 1940. Nat. Geosci. 5, 261–265. https://doi.org/10.1038/ngeo1421.
Pärn, J., Verhoeven, J.T.A., Butterbach-Bahl, K., Dise, N.B., Ullah, S., Aasa, A., Egorov, S., Espenberg, M., Järveoja, J., Jauhiainen, J., Kasak, K., Klemedtsson, L., Kull, A., Laggoun-Défarge, F., Lapshina, E.D., Lohila, A., Lõhmus, K., Maddison, M., Mitsch, W.J., Müller, C., Niinemets, Ü., Osborne, B., Pae, T., Salm, J.O., Sgouridis, F., Sohar, K., Soosaar, K., Storey, K., Teemusk, A., Tenywa, M.M., Tournebize, J., Truu, J., Veber, G., Villa, J.A., Zaw, S.S., Mander, Ü., 2018. Nitrogen-rich organic soils under warm well-drained conditions are global nitrous oxide emission hotspots. Nat. Commun. 9, 1135. https://doi.org/10.1038/s41467-018-03540-1.
Petersen, S.O., Hoffmann, C.C., Schäfer, C.M., Blicher-Mathiesen, G., Elsgaard, L., Kristensen, K., Larsen, S.E., Torp, S.B., Greve, M.H., 2012. Annual emissions of CH_4 and N_2O, and ecosystem respiration, from eight organic soils in Western Denmark managed by agriculture. Biogeosciences 9, 403–422. https://doi.org/10.5194/bg-9-403-2012.
Poyda, A., Reinsch, T., Kluß, C., Loges, R., Taube, F., 2016. Greenhouse gas emissions from fen soils used for forage production in northern Germany. Biogeosciences 13, 5221–5244. https://doi.org/10.5194/bg-13-5221-2016.
Rowland, C.S., Morton, R.D., Carrasco, L., McShane, G., O'Neil, A.W., Wood, C.M., 2017. Land Cover Map 2015 (25m Raster, GB). NERC Environmental Information Data Centre. https://doi.org/10.5285/bb15e200-9349-403c-bda9-b430093807c7.
Segers, R., 1998. Methane production and methane consumption: a review of processes underlying wetland methane fluxes. Biogeochemistry 41, 23–51. https://doi.org/10.1023/A:1005929032764.
Senbayram, M., Chen, R., Mühling, K.H., Dittert, K., 2009. Contribution of nitrification and denitrification to nitrous oxide emissions from soils after application of biogas waste and other fertilizers. Rapid Commun. Mass Spectrom. 23, 2489–2498. https://doi.org/10.1002/rcm.4067.
Sgouridis, F., Ullah, S., 2017. Soil greenhouse gas fluxes, environmental controls, and the partitioning of N_2O sources in UK natural and seminatural land use types. J. Geophys. Res. Biogeosci. 122, 2617–2633. https://doi.org/10.1002/2017JG003783.
Shaaban, M., Wu, Y., Khalid, M.S., Peng, Q.A., Xu, X., Wu, L., Younas, A., Bashir, S., Mo, Y., Lin, S., Zafar-ul-Hye, M., Abid, M., Hu, R., 2018. Reduction in soil N_2O emissions by pH manipulation and enhanced nosZ gene transcription under different water regimes. Environ. Pollut. 235, 625–631. https://doi.org/10.1016/j.envpol.2017.12.066.
Shaaban, M., Khalid, M.S., Hu, R., Zhou, Mi, 2022. Effects of water regimes on soil N_2O, CH_4 and CO_2 emissions following addition of dicyandiamide and N fertilizer. Environ. Res. 212, 113544 https://doi.org/10.1016/j.envres.2022.113544.
Shepherd, T.G., 2009. Visual soil assessment. In: Field Guide for Pastoral Grazing and Cropping on Flat Rolling Country, , 2nd ed.1. Horizons Regional Council, Palmerston North, New Zealand, p. 119.
Šimek, M., Jíšová, L., Hopkins, D.W., 2002. What is the so-called optimum pH for denitrification in soil? Soil Biol. Biochem. 34, 1227–1234. https://doi.org/10.1016/S0038-0717(02)00059-7.
Smith, K.A., Ball, T., Conen, F., Dobbie, K.E., Massheder, J., Rey, A., 2003. Exchange of greenhouse gases between soil and atmosphere: interactions of soil physical factors and biological processes. Eur. J. Soil Sci. 54, 779–791. https://doi.org/10.1111/ejss.12539.
Song, K., Zhang, G., Yu, H., Huang, Q., Zhu, X., Wang, T., Xu, H., Lv, S., Ma, J., 2021. Evaluation of methane and nitrous oxide emissions in a three-year case study on single rice and ratoon rice paddy fields. J. Clean. Prod. 297, 126650 https://doi.org/10.1016/j.jclepro.2021.126650.
Thompson, R.L., Lassaletta, L., Patra, P.K., Wilson, C., Wells, K.C., Gressent, A., Kof, E.N., Chipperfeld, M.P., Winiwarter, W., Davidson, E.A., Tian, H., Canadell, J.G., 2019. Acceleration of global N_2O emissions seen from two decades of atmospheric inversion. Nat. Clim. Chang. 9, 993–998. https://doi.org/10.1038/s41558-019-0613-7.
Thomson, B.C., Ostle, N.J., McNamara, N.P., Whiteley, A.S., Griffiths, R.I., 2010. Effects of sieving, drying and rewetting upon soil bacterial community structure and respiration rates. J. Microbiol. Methods 83, 69–73. https://doi.org/10.1016/j.mimet.2010.07.021.
Trost, B., Prochnow, A., Drastig, K., Meyer-Aurich, A., Frank, E., Baumecker, M., 2013. Irrigation, soil organic carbon and N_2O emissions. A review. Agron. Sustain. Dev. 33, 733–749. https://doi.org/10.1007/s13593-013-0134-0.
Ullah, S., Frasier, R., King, L., Picotte-Anderson, N., Moore, T.R., 2008. Potential fluxes of N_2O and CH_4 from soils of three forest types in eastern Canada. Soil Biol. Biochem. 40, 986–994. https://doi.org/10.1016/j.soilbio.2007.11.019.
van Lent, J., Hergoualc'h, K., Verchot, L.V., 2015. Reviews and syntheses: soil N_2O and NO emissions from land use and land-use change in the tropics and subtropics: a meta-analysis. Biogeosciences 12, 7299–7313. https://doi.org/10.5194/bg-12-7299-2015.
Volpi, I., Laville, P., Bonari, E., o di Nasso, N.N., Bosco, S., 2017. Improving the management of mineral fertilizers for nitrous oxide mitigation: the effect of nitrogen fertilizer type, urease and nitrification inhibitors in two different textured soils. Geoderma 307, 181–188. https://doi.org/10.1016/j.geoderma.2017.08.018.
Wan, Y., Ju, X., Ingwersen, J., Schwarz, U., Stange, C.F., Zhang, F., Streck, T., 2009. Gross nitrogen transformations and related nitrous oxide emissions in an intensively used calcareous soil. Soil Sci. Soc. Am. J. 73, 102–112. https://doi.org/10.2136/sssaj2007.0419.
Wang, J., Zhang, B.B., Tian, Y., Zhang, H., Cheng, Y., Zhang, J., 2018. A soil management strategy for ameliorating soil acidification and reducing nitrification in tea plantations. Eur. J. Soil Biol. 88, 36–40. https://doi.org/10.1016/j.ejsobi.2018.06.001.
Werner, C., Kiese, R., Butterbach-Bahl, K., 2007. Soil-atmosphere exchange of N_2O, CH_4 and CO_2 and controlling environmental factors for tropical rain forest sites in western Kenya. J. Geophys. Res. 112, D03308. https://doi.org/10.1029/2006JD007388.

Wilson, D., Farrell, C.A., Fallon, D., Moser, G., Müller, C., Renou-Wilson, F., 2016. Multiyear greenhouse gas balances at a rewetted temperate peatland. Glob. Chang. Biol. 22, 4080–4095. https://doi.org/10.1111/gcb.13325.

Wrage, N., Velthof, G.L., van Beusichem, M.L., Oenema, O., 2001. Role of nitrifier denitrification in the production of nitrous oxide. Soil Biol. Biochem. 33, 1723–1732. https://doi.org/10.1016/S0038-0717(01)00096-7.

Wu, L., Tang, S., He, D., Wu, X., Shaaban, M., Wang, M., Zhao, J., Khan, I., Zheng, X., Hu, R., 2017. Conversion from rice to vegetable production increases N_2O emission via increased soil organic matter mineralization. Sci. Total Environ. 583, 190–201. https://doi.org/10.1016/j.scitotenv.2017.01.050.

Xu, X., Yuan, X., Zhang, Q., Wei, Q., Liu, X., Deng, W., Wang, J., Yang, W., Deng, B., Zhang, L., 2022. Biochar derived from spent mushroom substrate reduced N_2O emissions with lower water content but increased CH_4 emissions under flooded condition from fertilized soils in Camellia oleifera plantations. Chemosphere 287, 132110. https://doi.org/10.1016/j.chemosphere.2021.132110.

Zhang, S., Yu, Z., Lin, J., Zhu, B., 2020. Responses of soil carbon decomposition to drying-rewetting cycles: a meta-analysis. Geoderma 361, 114069. https://doi.org/10.1016/j.geoderma.2019.114069.